

Fracture Behaviors of Metallocene-Catalyzed Polyethylene Elastomer via Silane Crosslinking

S.-M. Lai,¹ J.-L. Liu,¹ Y.-C. Chen,² K.-H. Chang²

¹Department of Chemical and Materials Engineering, National I-Lan University, I-Lan 260, Taiwan, Republic of China

²Department of Chemical Engineering, Chinese Culture University, Taipei 111, Taiwan, Republic of China

Received 22 December 2004; accepted 5 July 2005

DOI 10.1002/app.23524

Published online in Wiley InterScience (www.interscience.wiley.com).

ABSTRACT: Silane moisture-cured metallocene-catalyzed polyethylene (mPE) to form an elastomer has been prepared. Metallocene polyethylenes with two different levels of comonomer contents were grafted with various amounts of vinyltriethoxy silane. "Threshold" fracture energy is roughly proportional to the reciprocal square root of Young's modulus. By relating tensile strength to tear strength, the corrected average depth of flaw is in the range of $40.5 \pm 11.0 \mu\text{m}$, which successfully confirms the extension of conventional elastomeric theory to the low crystalline vulcanizates under some limitations. The cutting strength of

mPE vulcanizates gives an intermediate value when compared with crystalline plastics and conventional elastomer, and is comparable with other evaluations of cutting strength for different types of materials, which further signifies the importance of crystalline yielding even in the nano-fracture zone of deformation. © 2006 Wiley Periodicals, Inc. *J Appl Polym Sci* 101: 2472–2481, 2006

Key words: metallocene polyethylene (mPE); silane crosslinking; fracture behaviors; depth of flaw (natural flaw size)

INTRODUCTION

Thermoplastic elastomers (TPEs) generally possess elastomeric characteristic, yet can be efficiently processed as thermoplastics. Thus, TPEs have received much attention recently.¹ Major classes of TPEs include block copolymers, such as styrene–butadiene–styrene (SBS), and blends of elastomers with thermoplastics. To further upgrade the performance of TPE, a new generation of elastomer, metallocene polyethylene (mPE), is chosen here. In particular, mPE can be employed as TPE and conventional elastomer as well. When a low compression set is required, a complete cure of mPE should be imparted. This work was carried out to investigate the properties of this cured elastomer. The successful development of mPE is considered to be one of the most significant achievements in polymer history for the past 20 years.^{2–4} Numerous works have been devoted to new applications for this tailored unique polymer.

As metallocene polyethylene is a low-crystalline elastomer and is different from a conventional elastomer, factors to affect fracture behavior could be complicated such as, crystallinity, curing degree, mor-

phology, etc. No much details of work in the fracture behavior were investigated. Our earlier work has particularly elucidated the effect of the crosslinking types on the strength of polybutadiene and styrene–butadiene copolymer under a viscoelastic response.⁵ Fracture energy could be measured using tear test, etc. Threshold fracture energy under a minimized energy dissipation condition was proportional to the square root of the number average of the molecular weight between crosslinks for a C–C crosslinked elastomer.^{5–7} The deformation of a typical elastomer was characterized by a model of natural flaw size (edge crack) with an effective crack tip diameter. The strength of material was governed by the effective crack tip diameter varied with a viscoelastic condition.⁸ For crystalline material, the dissipation of material is not limited to a viscoelastic response. Enhanced energy dissipation is ascribed to factors from crystalline, filler, etc. Highly crystalline material like high-density polyethylene (HDPE) was studied to signify the importance of crystalline region on the strength of materials. Fracture zone of deformation in an order of spherulite size was deduced.^{9,10} Except for those conventional thermoplastics and amorphous elastomers that were studied, to the authors' knowledge, there is no literature available in discussing the aforementioned factors on the strength of the newly prepared postcured crystalline elastomer. The objective of this work is in attempt to apply the previous theories for the thermoplastic materials with a relatively low crystallinity like mPE. Most importantly, the evolution of

Correspondence to: S.-M. Lai (smlai@niu.edu.tw).

Contract grant sponsor: Grant-in-Aid from the R.O.C. Government; contract grant number: NSC 93-2216-E-197-001.

the depth of flaw using a similar approach in amorphous elastomeric materials has not been extended to this type of low crystalline elastomer before. Care should be taken to apply the previous theories in many aspects, such as the basic assumption of the conventional elastomer possessing elasticity.

Recently, some works were focused on the dynamical properties, rheological properties, and various types curing effects on mPE.^{11–13} For a silane cure approach, it is well known that this silane-cured technology was developed earlier in 1970 for conventional polyethylene.¹⁴ Silane cure products have been applied to the cable industry since then. Recent works have been devoted to silane-cured mPE in various applications. Shieh et al.¹⁵ have investigated water crosslinking reactions of silane-grafted polyolefin blends under static vulcanization. The crystallinity effect on the degree of crosslinking was discussed. One particular article regarding the formulation, morphology formation, property profiles, and processing characteristics for PP/mPE thermoplastic vulcanizate (TPV) was described by Fritz et al.¹⁶ This new TPV prepared via dynamic water crosslinking offers a colorless feature for the automotive application. Unfortunately, there was only a limit discussion on mechanical properties. Further work is in great need to understand the fracture behavior of this new type of vulcanizate.

In this study, mPE is chosen as a typical elastomer. MPE grafted with silane was prepared to obtain water-cured mPE vulcanizate. Both factors (crosslinking and crystallization) would affect the interfacial strength and ultimate properties of materials.^{5,17} The recently developed correlation of tear strength and tensile strength for the conventional elastomer would also be applied to derive a corrected depth of flaw for a thermoplastic elastomer like mPE for the first time.^{6,8} The effective crack tip diameter and threshold fracture energy were also calculated.^{18–22} The cutting test to confine a crack tip was carried out to signify the importance of the crack tip diameter.^{8,19,22} Several types of other polymers listed in the literature are summarized and compared to assess the effect of crystalline yielding for mPE vulcanizates.

EXPERIMENTAL

Materials

The materials used in this study were metallocene polyethylenes (mPEs). mPEs with a melt index of 1.0 were supplied from Dow Corporation under the trade names of EG8100 and EG8003, corresponding to octene comonomer contents (%) of 24 and 18, respectively. The initiator, dicumyl peroxide (DCP, Coin Akzo Nobel Co.), vinyl triethoxy silane (VTEOS, Fluka), and dibutyltin dilaurate (DBTL, Aldrich) are

reagent grade and used to impart silane grafting of mPE followed by a subsequent curing.

Sample preparations

The grafting reaction of mPE with various dosages of silane containing 0.1 phr of peroxide and 0.05 phr of the catalyst was carried out using an internal mixer (Brabender 815605, Plastograph) under 50 rpm for 10 min at 180°C. The resulting batches were hot pressed to form a thin sheet in a compression-molding machine. Curing was then effected and completed through a water bath for 4 h at the prescribed temperature of 80°C for most prepared samples. Note that a lower temperature of 50°C was used to activate water curing of mPE 8100 with a relatively low melting temperature to prevent a distortion of sample. Tensile test specimens complied with ISO-37 Type (III) standard were then prepared through a die cut. Trousers tear test specimens with a thickness of 1 mm were prepared with backing cloth at one side and with a center groove of 0.2 mm deep at both sides to guide a crack propagation. Thus, the thickness remained to be torn through is about 0.6 mm. Cutting test specimens with a thickness of 1 mm were also prepared with backing cloth at one side to prevent an extension of sample legs under load.

Measurements

Structure and thermal characterizations

The Infrared spectra for graft polymer were recorded on an attenuated total reflection spectrophotometer (Perkin-Elmer) at a resolution of 4 cm⁻¹ for 32 scans from 4000–650 cm⁻¹. The glass transition temperature (T_g) was determined via a dynamic mechanical analyzer DMA (Perkin-Elmer, DMA 7e) under a three-point bending mode at a frequency of 1 Hz at a heating rate of 5°C/min from -100 to 120°C. The melting temperature (T_m) was measured using a DSC (DuPont, TA2010) at a heating rate of 10°C/min from 5 to 200°C. The crystallinity was calculated by taking the heat of fusion divided by the enthalpy required for 100% crystallinity equal to 289 J/g here.²³ Continuous extraction of cured samples in boiling *p*-xylene (140°C) was carried out corresponding to ASTM D 2765-90 using a Soxhlet extraction method. Gel content was calculated by the ratio of the weight of dried insoluble samples and the weight of samples before swelling.

Rheological and mechanical tests

Rheological measurements were carried out using Gottfert 1501 to determine shear viscosity against shear rates ranging from 10 to 800(1/s) at 200°C. Tensile measurements were conducted based on ASTM-

D638 at a crosshead speed of 20 cm/min under various test temperatures ranging from room temperature to 110°C using a Universal Tensile Testing Machine model GY6040A4. Tensile strength, elongation, and yield strength were recorded. Energy density (U_b) under a stress–strain curve was determined as well. Trousers tear test was carried out in a similar condition to determine fracture energy (G_c) for this type of vulcanizate.

$$G_c = 2F/t \quad (1)$$

where F is the minimum force required to propagate a crack and t is the torn thickness.

The evaluation of effective edge crack depth (c) was calculated through the following equation:^{6,8}

$$G_c = U_b \times 2\pi c_0 = U_b \times c \quad (2)$$

where c_0 is the depth of the flaw and c is the effective edge crack depth.

Here, the effective edge crack depth is much larger than the crack tip diameter.

In addition, the cutting test was also employed to measure the fracture energy (G_c) using a razor blade at a cutting speed of 10 mm/min around room temperature. The schematic sketch of cutting test is shown in Figure 1. Pulling energy (P) and cutting energy (C) were calculated as follows:^{8,22}

$$P = 2f_A(1 - \cos\theta)/t \quad (3)$$

$$C = f/t \quad (4)$$

where f_A is the load, f is the cutting force, 2θ is the angle between two legs, and t is the cut thickness.

By measuring the cutting force and angle, the fracture energy G_c was calculated from the sum of energies expended in both pulling and cutting, that is,

$$G_c = P + C \quad (5)$$

RESULTS AND DISCUSSION

In this study, two types of mPEs were investigated. A representative mPE 8003 was presented unless otherwise stated. The authors have no intention to compare the strength of these two materials. The purpose of presenting two materials is to demonstrate the application of earlier theories for conventional elastomers (without crystalline effect) under some limitations to these newly prepared mPE vulcanizates with low crystallinity. Various types of properties including tensile strength, tear strength, and cutting strength were carefully correlated to derive natural flaw size and effective crack tip diameters.

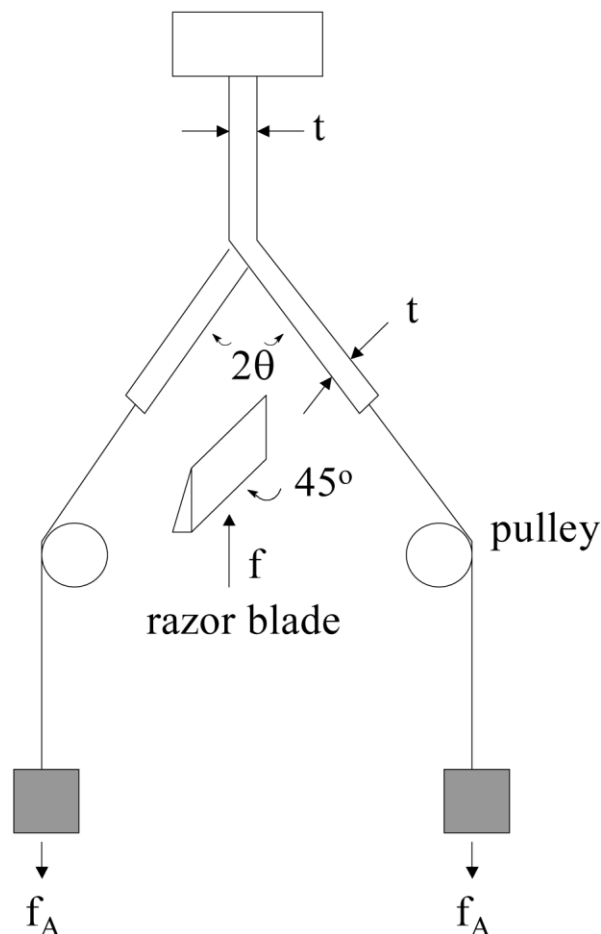


Figure 1 Schematic sketch of the cutting test.

Structure and thermal characterizations

To ensure a successful grafting reaction of silane onto mPE and have a better understanding on structure and thermal characteristics of mPE, the following measurements are performed on mPE resin. Taking mPE 8003 as representative material, the FTIR spectra of unmodified mPE and silane-grafted mPE8003 are depicted in Figure 2 for a comparison.²⁰ According to the literature,²⁴ the characteristic values of absorption bands range from 700–1200 cm^{-1} for silane grafting and crosslinking reaction. Thus, only this region is discussed here. As a result, the characteristic absorption bands of Si—O—C and Si—O—Si are specified at 1090 and 1030, respectively, which confirms silane grafting reaction and a subsequent silane crosslinking. Similar findings are also seen for mPE 8100 graft reaction.

After graft reactions, samples were subjected to subsequent crosslinking in the water bath. Gel levels were measured for each resin cured under different silane concentrations. Figure 3 shows gel contents for two types of mPE investigated in this study.²⁰ As the dosages of silane increase, gel contents increase and ap-

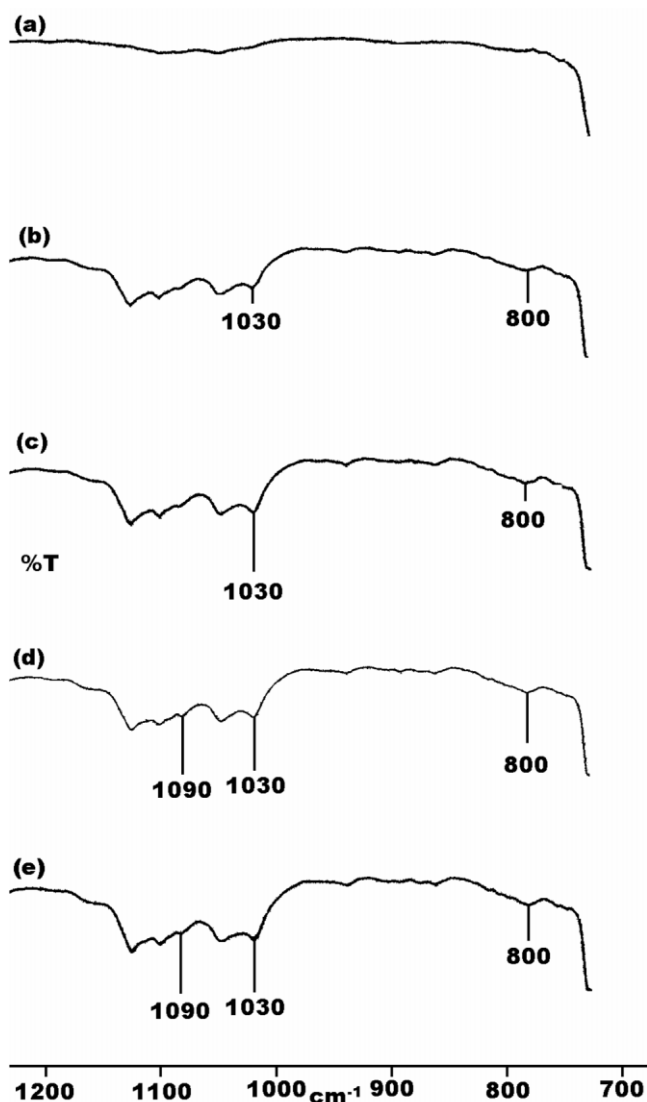


Figure 2 FTIR spectra of silane crosslinking of mPE 8003 modified with (a) 0 phr silane, (b) 0.5 phr silane, (c) 1.0 phr silane, (d) 2.0 phr silane, (e) 3.0 phr silane (0.1 phr DCP, 0.05 phr DBTL catalyst).²⁰

pear to level off at higher amounts of silane. Maximum values of gel content are attained at 71.8 and 77.8%, for mPE 8100 and mPE 8003, respectively. These values are in a similar order to those of silane crosslinking of conventional polyethylene.¹⁴ At the same dosage of silane concentration, mPE 8003 gives a higher degree of crosslinking efficiency. As several factors including comonomer content, comonomer distribution, molecular weight distribution, polydispersity, etc., are complicatedly involved, a concrete explanation is not given here. However, these results are in parallel to a peroxide cure system for both resins.

To investigate the effect of curing on the thermal behavior of mPE, the glass transition temperature (T_g), the melting temperature (T_m), the heat of fusion (ΔH),

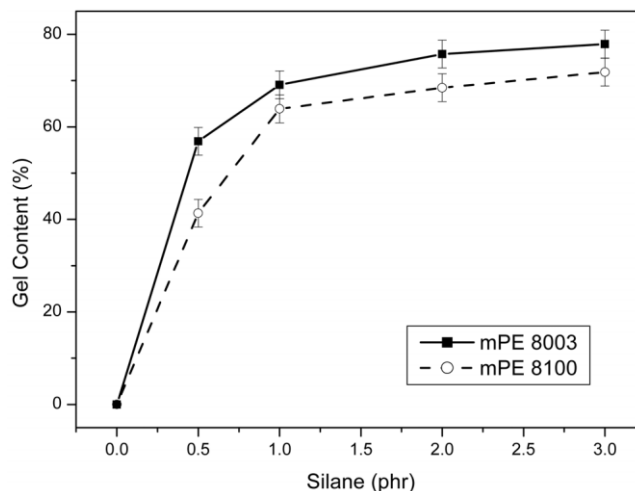


Figure 3 Gel contents of mPE 8100 and 8003 with different silane concentrations.²⁰

and the crystallinity recorded from a dynamic mechanical analyzer and differential scanning calorimetry are listed in Table I for mPE with various silane contents.²⁰ Taking mPE 8003 as an example, glass transition temperatures slightly increase from -45.7 to -41.4°C due to a possible constraint stemming from the silane curing effect. Additionally, no notable differences are found on the effect of degree of cure on the melting behavior and crystallinity. Presumably, the degree of cure attained in this system is not extremely high, as seen in other curing system such as a peroxide cure case. As for mPE 8100, similar effects are observed. Some of these results have been reported earlier in our other study.²⁰

Rheological properties

When mPE was grafted with silane to form mixing batches, torque values recorded from the internal

TABLE I
Thermal Analysis of mPE with Different Silane Contents²⁰

Silane (phr)	T_g ($^\circ\text{C}$)	T_m ($^\circ\text{C}$)	ΔH (J/g)	Crystallinity (%)
(a)mPE 8003				
0.0	-45.7	79.7	44.7	15.5
0.5	-42.6	78.7	43.3	15.0
1.0	-42.3	78.1	42.6	14.7
2.0	-41.6	77.9	42.4	14.7
3.0	-41.4	77.6	42.1	14.6
(b)mPE 8100				
0.0	-59.3	60.4	19.8	6.8
0.5	-59.1	59.8	18.4	6.5
1.0	-57.2	59.7	17.4	6.0
2.0	-56.3	59.5	17.1	5.9
3.0	-56.0	59.3	16.6	5.7

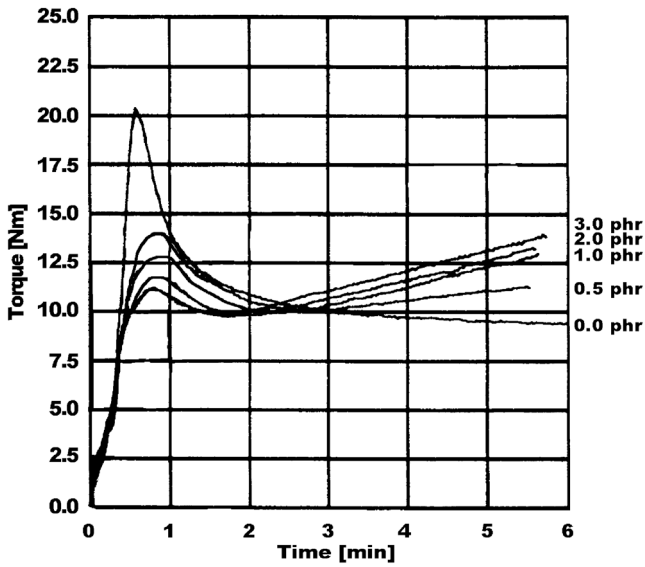


Figure 4 Mixing curves of mPE 8003 grafted with different silane concentrations.

mixer to monitor the progress of silane grafting reaction steadily increased with the level of silane concentrations, as shown in Figure 4. This is a dual effect resulting from an enhanced interaction between grafted silanes and a minor curing effect contributed from the Si—O—Si and C—C bond forming under heat and peroxide. The values of viscosities also indicate a similar trend. Viscosities of mPE 8003 grafted with different silane concentrations at various shear rates are shown in Figure 5. After a grafting reaction of mPE, the viscosity increases significantly up to four times when compared with the pristine mPE 8003. In addition, when the dosages of silane concentrations increase, the viscosity values appear to increase corre-

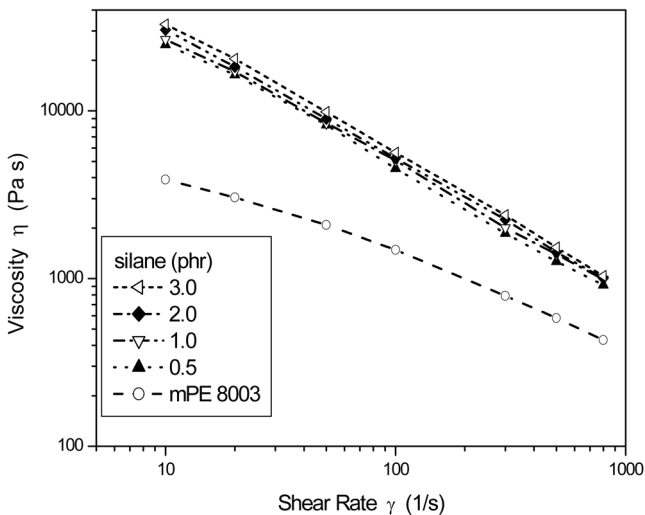


Figure 5 Viscosities of mPE 8003 grafted with different silane concentrations at various shear rates.

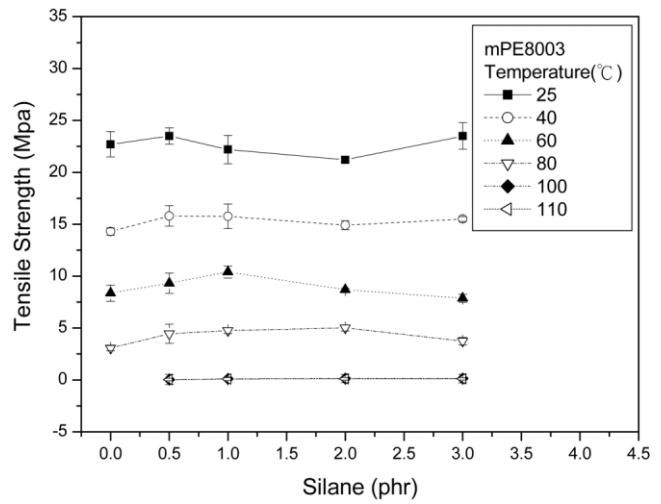


Figure 6 Tensile strength of mPE 8003 at various silane curing degrees under different test temperatures.

spondingly. Similar conclusion is also reached for mPE 8100 grafted with different silane concentrations.

“Threshold” fracture energy

Mechanical properties of the prepared vulcanizate were evaluated in an attempt to have a better understanding on the fracture behavior. Tensile strength of mPE 8003 elastomer at various silane curing degrees under different test temperatures is depicted in Figure 6. Tensile strength basically, as expected, decreases from 23.5 ± 0.8 MPa at 25°C to 0.034 ± 0.01 MPa at 110°C from a viscoelastic behavior point of view. As for the effect of curing degree, tensile strength varies slightly with increasing the levels of silane concentrations at all test temperatures. In the case when the crystalline region of mPE melts at the test temperature reaching 80°C, tensile strength tends to increase (not clearly shown here for brevity), which is probably due to an increase in gel content as seen in Figure 3 for gel measurements. Apparently, both crosslinking and crystallinity play important roles and mutually are affected by each other; these observations are more complicated at the temperature below the melting temperature. If one considers that the previous changes in crystallinity are marginal, the current results represent the sole effect of curing degree, especially at the temperature above melting temperature of mPE. As a matter of fact, when tensile strength was measured at the test temperature above 80°C, the phenomena became obvious.

To further compare the strength of this material, tear strength to measure fracture energy is evaluated. Figure 7 illustrates tear strength of a representative vulcanizate (mPE 8003) at various dosages of curing under different test temperatures. Tear strength de-

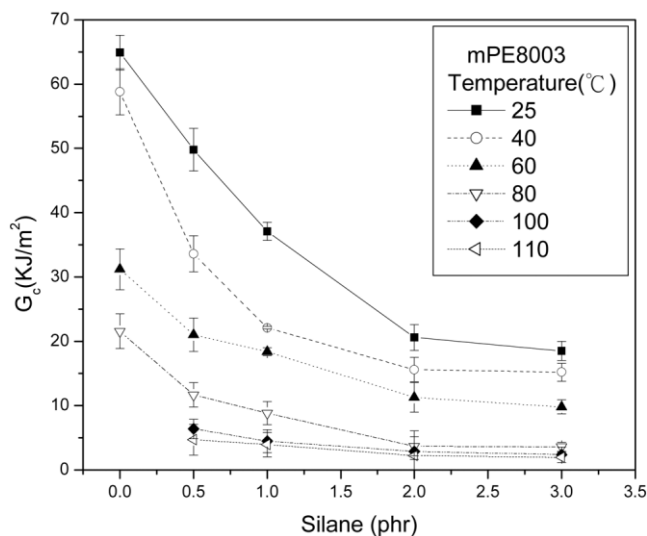


Figure 7 Tear strength of mPE 8003 at various silane curing degrees under different test temperatures.

creases with increasing test temperature as well. A significant drop at the temperatures above 60°C close to the melting temperature of mPE 8003 of ca. 80°C is observed. At a specific temperature, tear strength continues to decrease with increasing the degree of crosslinking. For instance, the difference of tear strength could vary from $64.9 \pm 2.7 \text{ kJ/m}^2$ (0 phr) to $18.5 \pm 1.5 \text{ kJ/m}^2$ (3.0 phr) at room temperature. Some data points are not available due to melting above 100°C for materials with a low degree of cure. As the degree of curing increases, the number of mobile chains between crosslinks in mPE decreases. This, in turn, reduces energy dissipation in deforming those molecular chains before one bond is broken to cause failure of test specimens.⁷ Again, if one could leave out the effect of marginal change in crystallinity, the sole effect of curing degree is clearly dominant in tear strength.

As crystalline regions also affect the strength of materials besides the crosslinking phenomena mentioned earlier, an attempt to rule out this effect is made to deliberately increase test temperatures above the melting temperature of mPE. With this arrangement, the effect from crystal deformation of mPE on tear strength is minimized. Fracture energy drops significantly up to one-tenth of values obtained at room temperatures. Contributions to the low strength of fracture energy are only from the crosslinking effect at high temperature. An attempt to quantitatively relate the tear strength to the modulus (an indication of degree of cure) measured at 110°C according to the theory developed by Lake and Thomas for an elastomer¹⁸ shows fair agreement.

In their study, threshold fracture energy of an elastomer with C—C crosslinks where energy dissipation is minimized is linearly proportional to the square

root of the molecular weight between crosslinks. According to the theory of elasticity, the molecular weight between crosslink is reciprocal to the modulus. Here, a rate dependent of the modulus at high temperature is minimized due to a reduced viscoelastic effect. So, Young's modulus was determined at the highest temperature (110°C) available for mPE 8003, because some of the results at higher temperatures are not available due to a low degree of cure to cause melting of materials. Representative results at the highest temperature termed the "threshold" fracture energy are thus plotted against the reciprocal square root of the modulus, shown in Figure 8. It appears that the linear relationship is roughly held under a reduced dissipation at this temperature for both resins. This slight deviation is rather understandable, because basically the degree of cure for this type of Si—O—Si is still not high (see gel content in Fig. 3). A portion of uncured molecular chain might flow significantly at high temperature, which causes the current theory to be invalid. This is based on the assumption that all bonds of one molecule between crosslink points must be stressed to break one. It is implied that the less the elastomer is crosslinked, the higher the value of the fracture energy. This accounts for the results of tear strength in Figure 7. Note that, at lower temperature, this linear relationship might not be valid. The reason of which is still the subject of interest in the field of fracture phenomena.

Corrected depth of flaw (natural flaw size): A correlation between tensile strength and tear strength

By relating tensile strength to tear strength, energy density is calculated and shown in Figure 9. Taking the results at room temperature, energy density does

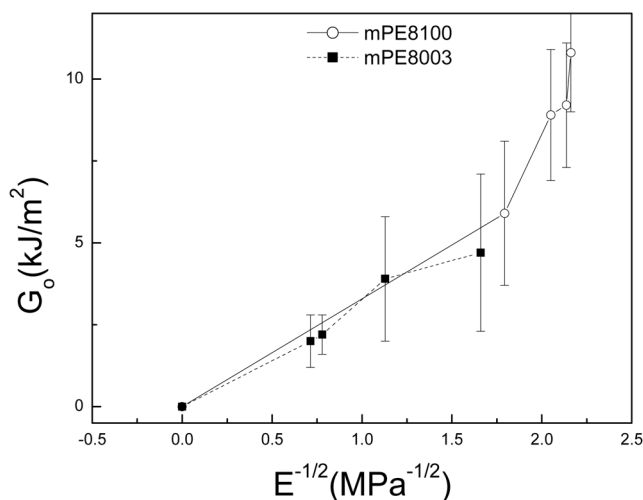


Figure 8 "Threshold" fracture energy plotted against the reciprocal square root of the modulus.

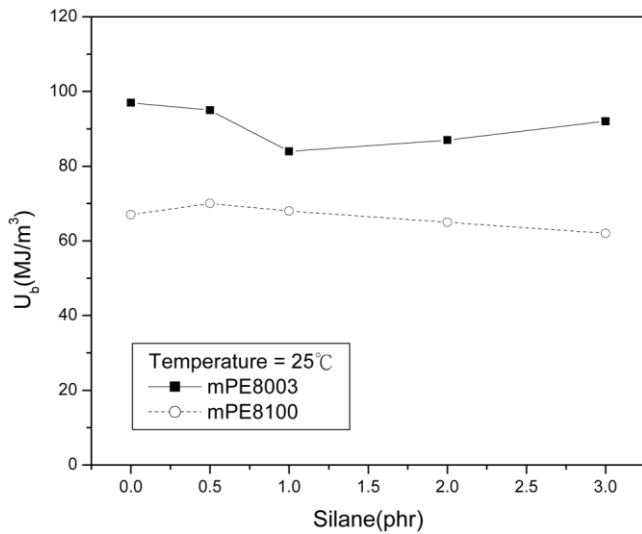


Figure 9 Energy density of mPE with different silane contents at 25°C.

not vary greatly with increasing the silane concentrations. In addition, the values of mPE 8003 are higher than those of mPE 8100. When a comparison is made at different temperatures, energy density decreases with test temperatures due to the aforementioned explanations for Figure 6.

To further understand the details of fracture phenomena for this vulcanizate, the flaw of depth deduced from the energy density and tear strength according to eq. (2) to test the previous theory is shown in Figure 10. These values decrease slightly with increasing silane concentrations, and tend to level off at the silane concentration above 2 phr. Also, when the comparison is made at other temperatures, the values of the depth of flaw vary widely. In some cases unreasonable numbers up to five times the previous measures occur above the melting temperature (not shown here for brevity). This is contradictory to a physical sense of the depth of the flaw, as the value should be independent of the test temperature. The reason to account for this observation is that the application of theory becomes invalid for the materials loss of elasticity. Both crystalline domains to cause severe dissipation and low degree of cure losing elasticity would be major limitations of the previous theory. Thus, at 0 phr of curing, the deviation from elastic behavior is noticeable. Thus, the corrected average depth of flaw should be determined at a relatively higher curing degree and low crystalline effect (but below the melting temperature of the resin), that is, 40°C for mPE8100 and 60°C for mPE 8003 at silane concentrations from 2 to 3 phr. However, to consider the experimental errors in measuring the strength of materials, all test temperatures below melting temperatures at silane dosage levels from 2 to 3 phr are considered. The corrected average depth of flaw is

thus in the range of $40.5 \pm 11.0 \mu\text{m}$. These values are close to the natural flaw size of $40 \pm 20 \mu\text{m}$ obtained from several different approaches.²¹ This concludes another possible approach in the extension of previous theory for conventional elastomer (without crystalline effect) to these newly developed low crystalline vulcanizate materials for the first time in the literature.

Effective diameters of fracture zone

To further give an insight of fracture phenomena for the novel vulcanizate, effective diameters of fracture zones deduced from intrinsic energy density and tear strength according to the following equation range from 13.0 to $0.4 \mu\text{m}$ for mPE8003 and from 9.8 to $0.2 \mu\text{m}$ for mPE8100, respectively, for test temperatures between room temperature and 110°C, if one takes intrinsic strength from the literature as $5 \text{ GJ}/\text{m}^3$.^{8,18,22,25} The values at higher temperatures generally follow a similar trend for tear strength. This correlation was established by Thomas.⁶

$$G_c = U_t * d \quad (6)$$

where U_t is the energy density at the crack tip and is an intrinsic strength of the material, and d is the crack tip diameter. The results at room temperature for both resins are illustrated in Figure 11 for a comparison. Effective crack tip diameters range from 13.0 to $3.7 \mu\text{m}$ for mPE8003 and from 9.8 to $1.7 \mu\text{m}$ for mPE8100, respectively, at room temperature. Basically, the crack tip diameters decrease with increasing silane contents. Similar treatments on the fracture zone were compared and gave an effective diameter of the order of $15 \mu\text{m}$ for HDPE and $18 \mu\text{m}$ for LDPE.¹⁰ Apparently, it comes to a good agreement based on this simple ap-

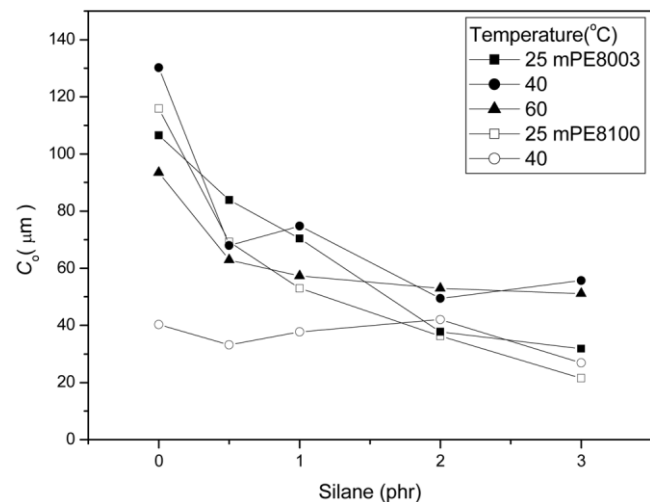


Figure 10 The depth of flaw of mPE with different silane contents at various temperatures.

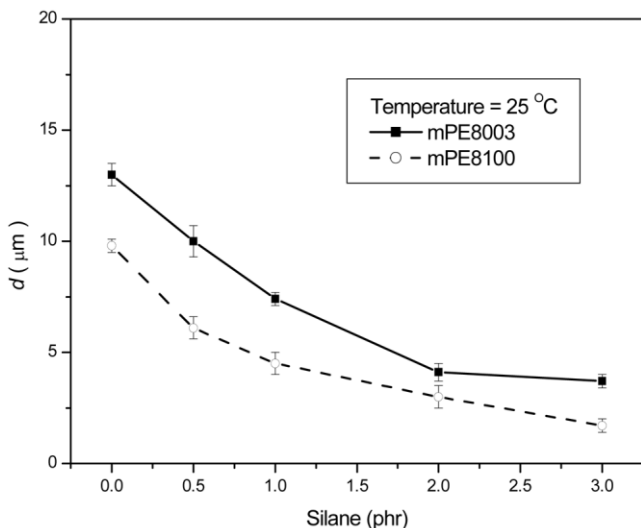


Figure 11 The effective crack tip diameter of mPE with different silane contents at 25°C.

proach. For a specific condition, tear strength to represent fracture energy is a characteristic property of the material. As tear strength changes in association to the rate of deformation and test temperature, the effective diameter varies corresponding to the viscoelastic behavior as well.⁸ As a result, the effective diameters change with the degree of cure.

To further confine the crack tip diameters at a nanoscale using a sharp razor blade, the cutting strength was evaluated. A typical curve of cutting strength for mPE8003 at 0 phr of silane is shown in Figure 12. A negative of slope of -1 is successfully drawn to obtain a cutting strength of 908 ± 62 (J/m^2), which indicates a good accordance of theory for this type of vulcanizate. The value is dramatically smaller

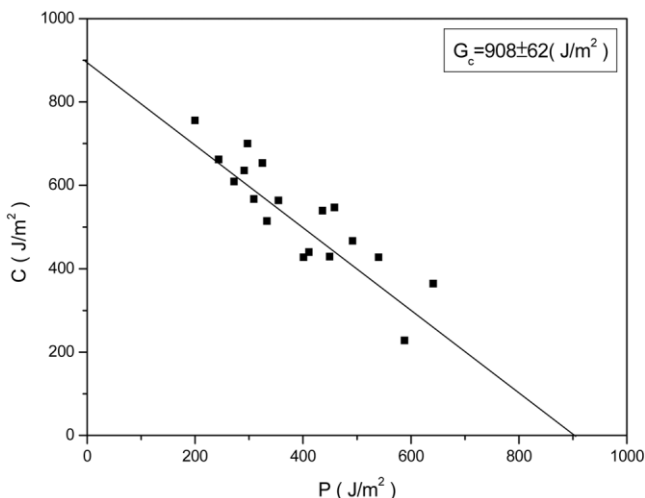


Figure 12 Cutting strength of mPE8003 (0 phr silane) at 25°C,

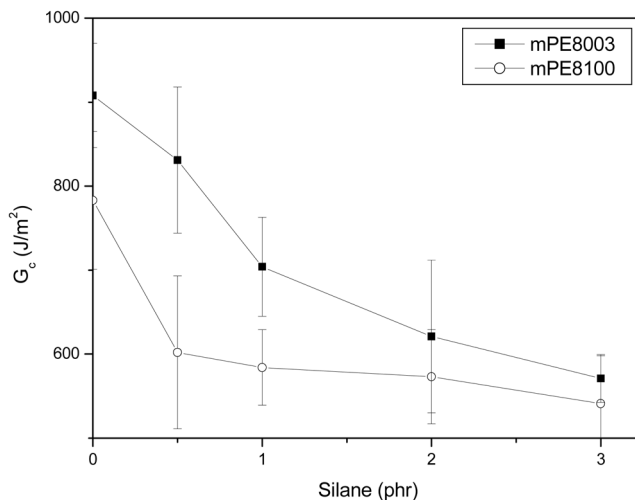


Figure 13 Cutting strength of mPE at various silane contents at 25°C.

than the tear strength of 64.9 ± 2.7 (kJ/m^2). The difference of fracture energy obtained in the two tests lies in the zone of fracture deformation (i.e., crack tip diameter, d) attained for different loading behavior. For the tear test the crack tip is not confined, as seen in the cutting test, depending on the blade tip diameter.

More measurements toward the comparison of cutting strength were carried out to reduce the macroyielding effect for two types of mPE vulcanizates. The results are depicted in Figure 13. The lowest value attained is ca. 541 ± 57 (J/m^2). Those values are not evaluated in the literature before but are comparable with other evaluations of cutting strength for different types of materials, for instance, HDPE,¹⁰ SBR,⁸ SBS,²⁵ and PP/EPDM TPV¹⁹ (see Table II). Lower values of cutting strength are normally observed for the conventional elastomer without crystalline effect, such as silicon rubber and SBR. Higher values of cutting strength for crystalline materials (LDPE and HDPE) indicate that a crystalline yielding effect still dominates the strength of material even using a blade to reduce the zone of deformation. A thermoplastic elastomer (SBS and mPE) displays the intermediate order of the cutting strength. In particular, cutting strength also decreases with increasing the degree of cure, which was demonstrated using cured mPE and SBS. Because the blade tip should be the same as the crack tip diameter on behalf of this cutting design, the crack tip diameter seems to change according to the previous manner. Accordingly, induced yielding from the blade is surmised and possible. An attempt to reduce all the energy dissipation from crystalline region is not possible in the current cutting design.

Note that previous comparisons on tensile strength and tear strength to yield the effective edge crack depth show large scatters at higher temperature. Measurements of cutting strength at other test tempera-

TABLE II
Cutting Strength of Various Types of Polymers

Polymer types	Examples	G_c (J/m ²)	Reference
Conventional elastomer	Silicon rubber	70	10
	Styrene-butadiene rubber (high styrene content) crosslinked with 0.5 phr DCP	250 ± 15	8
	Styrene-butadiene rubber (high styrene content) crosslinked with 2.5 phr DCP	140 ± 10	8
Thermoplastic elastomer	Styrene-butadiene-styrene copolymer (SBS)	570 ± 20	25
	SBS crosslinked with 0.1 phr DCP	375 ± 12	25
	PP/EPDM (Santoprene)	970 ± 65	19
	Two metallocene PEs (mPE) with different crystallinity	908 ± 62, 783 ± 82, 571 ± 29,	This work
	Two mPEs crosslinked with 3 phr silane	541 ± 57	This work
Semicrystalline plastics	LDPE	1000 ± 200	10
	HDPE	4000 ± 500	10

tures are therefore not discussed here, and will be discussed in a separate study. However, it does reduce the zone of deformation to a certain degree when compared with tear measurements. If one takes intrinsic strength as 5 GJ/m³ from the literature,^{8,18,22,25} the effective diameter seems to range from 0.18 to 0.11 μm for mPE8003 vulcanizate, and 0.16 to 0.10 μm for PP/mPE8100. These values are close to estimated blade diameter of ca. 0.1 μm at the room temperature in a controlled manner and are about two orders of magnitude smaller than results from tear measurements. Apparently, these values are in a measure of the extent of plastic yielding around the tear tip, and good agreements are reached for this newly developed vulcanizate.

Energy dissipation: A comparison of tear strength and cutting strength

As reported in our previous study, the higher the energy dissipation the higher the strength.⁵ The strength is predominately governed by the energy dissipation process, such as viscoelastic process, crystalline yielding effect, etc., which determines the magnitude of effective crack tip diameter. The difference of tear strength and cutting strength lies in the zone of fracture deformation (i.e., crack tip diameter, d) attained for different loading behavior. For the tear test, the crack tip is not confined, as seen in the cutting test, depending on the blade tip diameter. When the test temperature increases in the case of the tear test, the crack tip diameter decreases. Even in the case of "threshold" fracture energy (the lowest measurable tear strength) for mPE vulcanizates, the values are in an order of kJ/m² and are still higher than those values of few hundred J/m² obtained at cutting test (see Figs. 8 and 13). As discussed earlier, the blade tip diameter is in the order of 0.1 μm. Apparently, the

fracture zone of deformation attained for tear measurement for low crystalline and low crosslinked mPE vulcanizate is still higher than that for the cutting measurement. On the other hand, the "threshold" fracture energy is lower than that of the cutting strength in our previous study for highly crosslinked SBR without a crystalline effect.⁸ Those differences again are attributed to the energy dissipation process. A high crosslinking degree of elastomer without a crystalline yielding effect gives low fracture energy. Here, mPE vulcanizates with a low crosslinked degree as well as a low crystalline yielding effect confers higher fracture energy unless a limited controlled crack tip diameter is enforced as seen in the cutting measurement. The strength of materials was clearly dominated more by the crystalline yielding effect than the viscoelastic effect, even in this nano-fracture zone of deformation.

CONCLUSIONS

Silane moisture-cured metallocene polyethylene to form a novel vulcanizate has been prepared. FTIR has been employed to confirm the graft reaction of silane. As for the effect of curing degree, the tensile strength varies slightly with increasing the levels of silane concentrations at all test temperatures. Tear strength generally decreases with reduced energy dissipation at a higher degree of cure. Representative results at the highest temperature termed "threshold" fracture energy appear to be linearly proportional to the reciprocal square root of modulus under reduced energy dissipation for both resins. By relating tensile strength to tear strength, the corrected average depth of flaw (natural flaw size) is in the range of 40.5 ± 11.0 μm, which agrees with the values obtained from several different approaches for conventional elastomers.

Note that the depth of flaw should be determined at relative higher curing degree and low crystalline effect (but below melting temperature of the resin) to fulfill the assumption of earlier theory for elastomeric materials. Under this careful treatment, the application of Rivlin and Thomas's theory has been successfully extended to this newly developed low crystalline vulcanizate for the first time in the literature. The effective diameters of fracture zones deduced from intrinsic energy density and tear strength are in an order of few micromoles at room temperature. Cutting strength of mPE vulcanizates gives an intermediate value when compared with crystalline plastics and a conventional elastomer. Those values are generally two orders of magnitude smaller than the results from tear measurements. The strength of materials was clearly dominated by the crystalline yielding effect more than the viscoelastic effect, even in this nano-fracture zone of deformation for low crystalline mPE vulcanizates.

References

1. Holden, G.; Legge, N. R.; Quirk, R. P.; Schroeder, H. E., Eds.; *Thermoplastic Elastomer*; Hanser: Munich, 1996.
2. Technical Brochure, DuPont Dow Elastomer, Inc., 1993.
3. Fritz, H. G. *Polymer Processing Society, PPS-14, Japan, 1998*; p 3.
4. Spontak, R. J.; Patel, N. P. *Curr Opin Coll Interface Sci* 2000, 5, 334.
5. Gent, A. N.; Lai, S.-M. *J Polym Sci Polym Phys* 1994, 32, 1543.
6. Rivlin, R. S.; Thomas, A. G. *J Polym Sci* 1953, 10, 291.
7. Thomas, A. G. *J Polym Sci* 1955, 18, 177.
8. Gent, A. N.; Lai, S.-M.; Nah, C.; Wang, C. *Rubber Chem Technol* 1994, 67, 610.
9. Gent, A. N.; Jeong, J. *J Mater Sci* 1986, 21, 355.
10. Gent, A. N.; Wang, C. *J Polym Sci Polym Phys* 1996, 34, 2231.
11. Nitta, K. H.; Tanaka, A. *Polymer* 2001, 42, 1219.
12. Aguilar, M.; Vega, J. F.; Sanz, E.; Martinez-Salazar, J. *Polymer* 2001, 42, 9713.
13. Kummer, K. G.; Edmondson, M. S.; Hayes, J. W.; Parikh, D. R. Paper 19, 152nd Rubber Division, ACS, 1997.
14. Scott, H. G. U.S. Pat. 3,646,155 (1972).
15. Shieh, Y.-T.; Chuang, H.-C.; Liu, C.-M. *J Appl Polym Sci* 2001, 81, 1799.
16. Fritz, H. G.; Bolz, U.; Cai, Q. *Polym Eng Sci* 1999, 39, 1087.
17. Gent, A. N.; Schultz, J. *J Adhes* 1972, 3, 281.
18. Lake, G. J.; Thomas, A. G. *Proc R Soc (Lond)* 1967, A300, 108.
19. Wang, C.; Chang, C.-I. *J Appl Polym Sci* 2000, 75, 1033.
20. Lai, S.-M.; Hu, N.-H.; Chen, W.-C.; Wang, D. S.-T. *J Polym Sci Eng*, submitted.
21. Gent, A. N. In *Science and Technology of Rubber*; Eirich, F. R. Ed.; Academic Press: New York, 1978; Chapter 10.
22. Lake, G.-J.; Yeoh, O. H. *J Polym Sci Polym Phys* 1987, 25, 1157.
23. Chandra, R.; Rustgi, R. *Polym Degrad Stabil* 1997, 56, 185.
24. Hjertberg, T.; Palmolf, M.; Sultan, B.-A. *J Appl Polym Sci* 1991, 42, 1185.
25. Wang, C.; Chang, C.-I. *J Polym Sci Polym Phys* 1997, 35, 2003.